The Polar Nano Regions ⇌ Relaxor Transition in $Pb_{1-X}(Sc_{1/2}Nb_{1/2})O_{3-X}$; $X = bulk\ concentration\ of\ nearest\ neighbor\ [Pb-O]\ divacancies$.

B. P. Burton, D. B. Gopman, and Gunay Dogan
Materials Science and Engineering Division, Materials Measurement Laboratory, National Institute of Standards and Technology Gaithersburg, MD 20899-8520, USA

Eric Cockayne
Materials Measurement Science Division, Materials Measurement Laboratory, National Institute of Standards and Technology Gaithersburg, MD 20899-8520, USA

Sarah Hood
Materials Science and Engineering Division, Materials Measurement Laboratory, National Institute of Standards and Technology Gaithersburg, MD 20899-8520, USA and Hood College, Frederick, MD 21701, USA

arXiv:1612.00398v1 [physics.comp-ph] 1 Dec 2016

In previous work, molecular dynamics simulations based on a first-principles-derived effective Hamiltonian for $Pb_{1-X}(Sc_{1/2}Nb_{1/2})O_{3-X}$ (PSN), with nearest-neighbor Pb-O divacancy pairs, was used to calculate $X_{[\mathrm{Pb-O}]}$ vs. T, phase diagrams for PSN with: ideal rock-salt type chemical order; nanoscale chemical short-range order; and random chemical disorder. Here, we show that the phase diagrams should include additional regions in which a glassy relaxor-phase (or state) is predicted. With respect to phase diagram topology, these results strongly support the analogy between relaxors and magnetic spin-glass-systems.

PACS numbers: 77.80.Bh, 77.84.Dy, 64.70.Kb, 61.46.-w

Submitted for publication in Physical Review B, December 2, 2016

INTRODUCTION

Heterovalent perovskite-based $Pb(B,B')O_3$ relaxor ferroelectrics (RFE) [1, 2], such as $Pb(Sc_{1/2},Nb_{1/2})O_3$ (PSN), $Pb(Sc_{1/2},Ta_{1/2})O_3$ (PST), and $Pb(Zn_{1/3},Nb_{2/3})O_3$ (PZN) and, *relaxors* [which have no ferroelectric (FE) ground-state] such as $Pb(Mg_{1/3},Nb_{2/3})O_3$ (PMN) and $Pb(Mg_{1/3},Ta_{2/3})O_3$ (PMT), are technologically important transducer/actuator materials with extraordinary dielectric and electromechanical properties. Chemically disordered PSN exhibits polar nano-regions (PNR) characteristics (more polarizable PNR in a less polarizable matrix) above a normal FE-transition at T_{FE} ≈373 K. Chu *et al.* [3] demonstrated that the addition of 1.7 atomic % Pb-O divacancies depresses the FE transition temperature (T), from T_{FE} ≈373 K to T_{FE} ≈338 K, and broadens the T-range in which PNR properties, *e.g.* frequency dispersion in the dielectric response, are observed. Chu *et al.* also reported similar and more complete results for isostructural PST[4–6]. These results suggest that a sufficient bulk concentration of divacancy pairs, $X_{[\mathrm{Pb-O}]}$, will drive the system to a relaxor ferroelectric (RFE) state, with an FE-ground-state, or to a fully relaxor state, without an FE-ground-state, at $X_C < X_{[\mathrm{Pb-O}]}$, where X_C is the critical composition at which $T_{FE} \to 0K$.

Chemical disorder and defects such as Pb-vacancies (V_{Pb}) [7], oxygen vacancies (V_O) or charge-compensating nearest neighbor (nn) Pb-O divacancy pairs (V^{nn}_{Pb-O}) [8], are sources of local, *random fields* ($\vec{h_i}$) e.g. [9–11] (angle brackets indicate a simulation box average). Hence, the T vs. $X_{[\mathrm{Pb-O}]}$ phase diagrams presented here are topologically equivalent to the T vs. $\langle\vec{h_i}\rangle$ diagrams that are typically drawn for analytical mean-field models of magnetic spin-glass (SG) systems [12–15].

Recent publications by Sherrington [12–15] emphasized an analogy between relaxor ferroelectrics and magnetic SG with $soft-pdeudospins$; *i.e.* magnetic spins or ferroelectric displacements with variable magnitudes and arbitrary orientations. Pseudospin-psuedospin interactions in these models are frustrated (random-bond frustration [16]), and the combination of frustration plus quenched chemical disorder [17] are identified as essential constituents of relaxors. The model used here: also has *soft pseudospins* (ξ_i) at each Pb-site; first-, second-, and third-nn $\xi_i - \xi_j$-pairwise interactions, plus 4'th through 39'th-nn $\xi_i - \xi_j$-pair dipole-dipole interactions; and $\vec{h_i}$ at each Pb-site. An analysis of $\vec{h_i}$ that is based on nn Pb–B-site pairs in an ideal perovskite structure with a random cation configuration [11] indicates a distribution of orientations such that 34% are along < 111 >-type directions; 21% are < 001 >-type;

19% are < 110 >-type; 19% are < 113 >-type; and 7% are < 000 >[11] (weighted by $\vec{h_i}$-strength the corresponding percentages are: 29% < 111 >, 21% < 001 >, 23% < 110 >, and 27% < 113 >). The $\vec{h_i}$ used for the calculations presented here were calculated as the local field imposed by the whole simulation box. In this model, $\xi_i - \xi_j$ pairwise interactions are all FE in character, hence the $\vec{h_i}$ and [Pb-O]-divacancies are the only sources of frustration; and ideally NaCl-ordered pure PSN is unfrustrated.

Results presented here require changes in the phase diagrams that were presented in [18]. The field that was formerly referred to as the RFE-region in $T(\mathrm{X}_{[\mathrm{Pb-O}]})$ vs. phase diagrams [18] is now divided into: 1) a PNR-region, in which spatially static but orientationally dynamic PNR (centered on ≈2 nm diameter chemically ordered regions [19]) are embedded in a less polarizable matrix; and 2) an RFE/relaxor-region ($relaxor-region$ for brevity) in which PNR have more static orientations. The $\mathrm{T}(X_{[\mathrm{Pb-O}]})$-curve [*i.e.* $\mathrm{T}(\langle\vec{h_i}\rangle)$-curve] that divides the PNR-region from the relaxor-region is referred to as $T^{\bigstar}(X_{[\mathrm{Pb-O}]})$. Dkhil [20] referred to $T^{\bigstar}$ as "...a local phase transition that gives rise to the appearance of static polar nanoclusters." We reject the phrase "local phase transition," because (strictly) phase transitions only occur in infinite systems, and because our results suggest a weakly first-order transition, however, we do predict a subtle stiffening of PNR-orientations below $T^{\bigstar}$.

In previous simulations[11, 18], the presence of V_{Pb} vacancies[7] or V^{nn}_{Pb-O} divacancies[11, 18] in PSN lead to more diffuse FE phase transitions, with broadened dielectric susceptibility peaks; however, the RFE/relaxor-phase (state?) was not clearly delineated. Here, simulations are used to construct $X_{[\mathrm{Pb-O}]}$ vs. T phase diagrams for $Pb_{1-X}(Sc_{1/2}Nb_{1/2})O_{3-X}$ with random, perfectly rock-salt ordered and nano-ordered (NO) cation configurations as in [18]. The NO configuration has 20 NaCl-type ordered clusters in a percolating random matrix. Divacancy concentration- and T-ranges for PE- and FE-phases, and for "RFE-states", were identified from changes in polarization correlations[21], but the RFE/relaxor-phase *per se* was not delineated.

SIMULATIONS

The Model Hamiltonian

Simulations were performed using the first-principles based effective Hamiltonian H_{eff} that is described in detail in [11]; it expands the potential energy of PSN in a Taylor series about a high-symmetry perovskite reference structure, including those degrees of freedom relevant to FE phase transitions:

$$\begin{aligned} H_{eff} &= H(\{\vec{\xi_i}\}) + H(e_{\alpha\beta}) + H(\{\vec{\xi_i}\}, e_{\alpha\beta}) + PV \\ &+ H(\{\vec{\xi_i}\}, \{\sigma_l\}, \{\mathrm{V}_{\mathrm{Pb-O}}\}) \end{aligned} \quad (1)$$

where $\{\vec{\xi_i}\}$ represents Pb-site centered local polar distortion variables of arbitrary magnitudes and orientations; $e_{\alpha\beta}$ is a homogeneous strain term; $H(\{\vec{\xi_i}\}, e_{\alpha\beta})$ is a strain coupling term; and PV the standard pressure-volume term. The first four terms are sufficient to model pressure-dependent phase transitions in a normal FE perovskite without local fields [22]. The fifth term, $H(\{\vec{\xi_i}\}, \{\sigma_l\}, \{\mathrm{V}_{\mathrm{Pb-O}}\})$, represents coupling between polar variables and "random" local fields, $\vec{h_i}$, [11, 23, 24] from: 1) screened electric fields from the quenched distribution of Sc^{3+} and Nb^{5+} ions $\{\sigma_l\}$; and 2) by $\mathrm{V}_{[Pb-O]}$.

As described in [18] all simulations were done with a $40\times40\times40$ MD-supercell, in which each Pb-atom is associated with a local distortion vector, $\vec{\xi_i}$, that indicates the displacement of lead atom Pb_i from its ideal perovskite position. The effective Hamiltonian in Eqn. 1 was used to derive equations of motion, with an MD time-step of 0.06 picoseconds.

Divacancies are modeled by replacing $40^3 X_{[\mathrm{Pb-O}]}$ randomly selected local distortion variables with fixed dipole moments corresponding to V^{nn}_{Pb-O} divacancy pairs (*i.e.* local fields directed, from a Pb-site, along one of the 12 ⟨110⟩-type vectors).

Order Parameters

Curves for the Burns temperatures, $T_B(X_{[\mathrm{Pb-O}]})$, [25] and the FE-transitions, $T_{FE}(X_{[\mathrm{Pb-O}]})$ are identical to those in [18]. Curves for $T^{\bigstar}(X_{[\mathrm{Pb-O}]})$ were located by plotting T-dependent $q_{\xi\xi}$- and $q_{\Delta t}$-curves where: $q_{\xi\xi}$ is the self-overlap order parameter, [26] Eqn. 2; and $q_{\Delta t}$ Eqn. 3, is an autocorrelation function that compares the displacement of atom ξ_i at time-t with ξ_i at time-$t+\Delta t$ (typically, Δt = 100 MD-snapshots = 6.0 picoseconds).

The idea behind $q_{\Delta t}$ is that a time-sensitive order parameter may be more sensitive to the sort of PNR-stiffening referred to by Dkhil: [20]

$$q_{\xi\xi} = \frac{1}{N}\sum_i \langle \vec{\xi}_i \cdot \vec{\xi}_i \rangle \tag{2}$$

and

$$q_{\Delta t} = \frac{1}{N}\sum_i \langle \vec{\xi}_{i,t} \cdot \vec{\xi}_{i,t+100} \rangle \tag{3}$$

where: N is the number of Pb-sites; summations are over the all Pb-displacements; and the averaging represented by angle brackets is over the last 1000 MD-snapshots in a 3000- or 5000 snapshot series (see below). Within the precision of these simulations, both order parameters yield the same results for $T^{\bigstar}(X_{[\mathrm{Pb-O}]})$.

Numerical simulations can not distinguish between crossovers and phase transitions where: crossovers correspond to inflection points in $q_{\xi\xi}(T)$ and/or $q_{\Delta t}(T)$; and phase transitions correspond to discontinuities in first- or second-T-derivatives of $q_{\xi\xi}(T)$ and/or $q_{\Delta t}(T)$ (*i.e.* first-order, or continuous- or critical-transition, respectively [27]). Because the results for random- and NO-cation configurations strongly suggest a (weakly) first-order phase transition, $T^{\bigstar}$ will be referred to as a phase *transition*, and the relaxor will be referred to as a *phase*, but with the caveat that $T^{\bigstar}$ may actually mark a crossover, and the relaxor would then be a *state*.

Order parameter values were calculated from MD-snapshots that were taken every 100 MD time-steps in a series of 3000 or 5000 MD-snapshots (enough snapshots that $q_{\xi\xi}(T)$ and $q_{\Delta t}(T)$, are approximately constant for 1000 snapshots); 3000 for the NaCl-ordered and random cation configurations; 5000 for the NO configuration. Plotted order-parameter values are averages over the last 1000 MD snapshots in a series.

RESULTS

Representative results for order-parameter vs. T curves are plotted in Figs. 1, 2, and 3. Corresponding phase diagrams are plotted in Figs. 4. In all these plots, T is normalized by T^0_{FE}, the ferroelectric transition temperature (T_{FE}) of pure ideally rock-salt-ordered $Pb(Sc_{1/2}Nb_{1/2})O_3$. Vertical lines in Figs. 1, 2, and 3 indicate previously determined [18] values for T_{FE} and T_B. In all these Figures: T_{FE} is plotted as a solid line (blue online); T_B is plotted as a dashed line (blue online); and $T^{\bigstar}$ is plotted as a dotted lines (red online). In Figs. 4, large asterisk-symbols indicate points at which $T^{\bigstar}$ was located in $q_{\xi\xi}(T)$- and $q_{\Delta t}(T)$-curves.

With decreasing T, $q_{\xi\xi}(T)$ and $q_{\Delta t}(T)$ typically exhibit: broad minima at or near T_B; smooth monotonic increase in the PNR-region between $T^{\bigstar}$ and T_B; and erratic increase in the relaxor-region below $T^{\bigstar}$. The erratic characters of $q_{\xi\xi}(T)$- and $q_{\Delta t}(T)$-curves in the relaxor-regions of random- and NO-cation-configurations are interpreted as indicating glassy behavior. In particular, Figs 3b, which shows the MD time-dependence of $q_{\Delta t}(T)$, indicates that in the PNR-region above $T^{\bigstar}$ $q_{\Delta t}(T)$ evolves monotonically, however, in the relaxor-region below $T^{\bigstar}$, $q_{\Delta t}(T)$ passes through local minima before finding what we take to be its final value; as one expects for a glassy material.

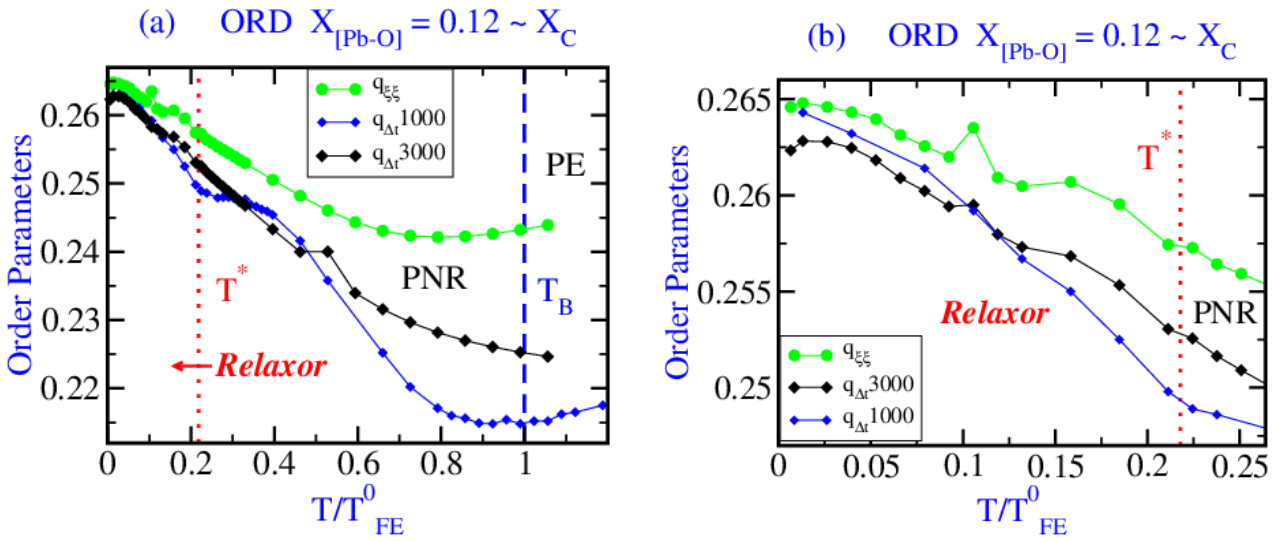

FIG. 1: Order parameters that were used to define the relaxor-region in $Pb_{1-X}(Sc_{1/2}Nb_{1/2})O_{3-X}$, with ideal rock-salt type Sc:Nb-chemical order: $q_{\xi\xi}(T)$ is the self-overlap order parameter (Eqn. 2); and $q_{\Delta t}$ (Eqn. 3) is a temporal autocorrelation function ($q_{\Delta t}1000$ and $q_{\Delta t}3000$ are results from 1000- and 3000-snapshots, respectively). Panels: (a) is the full diagram; (b) is an enlargement of the low-T portion of the diagram. Here, $T^{\star}$ looks as though it may mark a continuous transition, or a crossover.

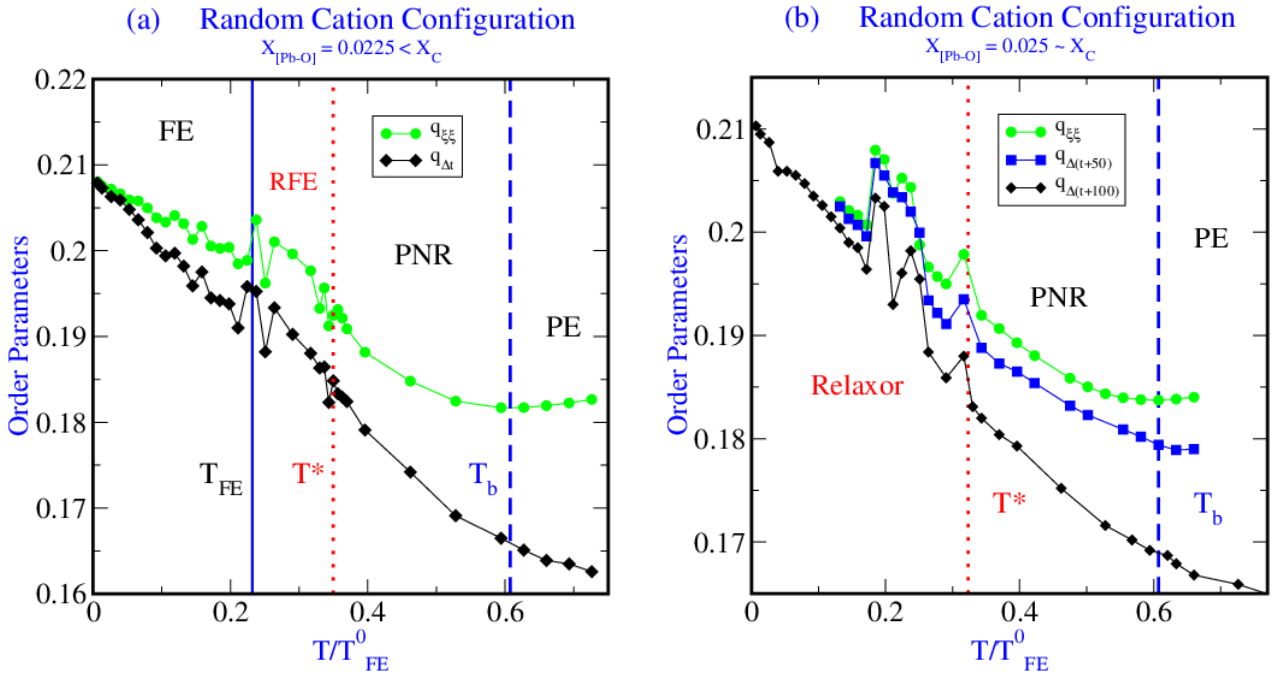

FIG. 2: Order parameters as functions of temperature for $Pb_{1-X}(Sc_{1/2}Nb_{1/2})O_{3-X}$, with a random Sc:Nb-cation configuration. $q_{\xi\xi}(T)$ and $q_{\Delta t}(T)$ (defined in Eqns. 2 and 3): (a) $X_{[\mathrm{Pb-O}]} = 0.0225 < X_C$ where there is a relaxor ferroelectric (RFE) with an FE-ground-state; (b) $X_{[\mathrm{Pb-O}]} = 0.025 \approx X_C$ has no FE-ground-state. In both (a) and (b), $T^{\star}$ appears to mark a weakly first-order transition (an $\approx 3\%$ discontinuity). In (b) $q_{\xi\xi}(T)$, $q_{t+50}(T)$, and $q_{t+100}(T)$ exhibit only small quantitative differences.

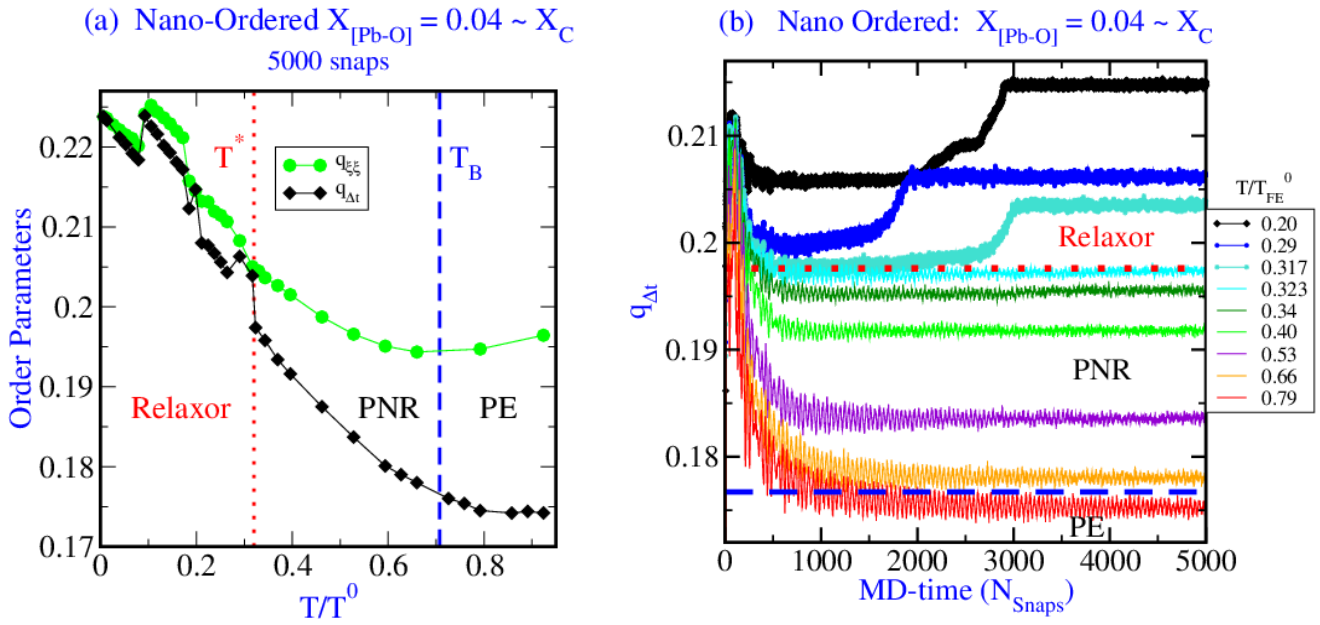

FIG. 3: Order parameters as functions of temperature for a nano-ordered Sc:Nb-cation configuration of $Pb_{1-X}(Sc_{1/2}Nb_{1/2})O_{3-X}$, with 25% ordered regions in a random matrix: (a) $T^{\bigstar}$ appears to mark a weakly first-order phase transition (an $\approx 1\%$ discontinuity in $q_{\xi\xi}$ or $\approx 2\%$ in $q_{\Delta t}$); (b) is a plot of $q_{\Delta t}$ as a function of time, where N_{snaps} is the number of snapshots in a 5000 snapshot series. At $T < T^{\bigstar}$, above the horizontal dotted line (red online), the system traverses local minima before converging.

Ideal Rock-Salt Chemical Order

Unlike the random- and nano-ordered cation configurations, the PNR⇌relaxor *transition* is subtle in the ideally NaCl-ordered system; in which [Pb-O]-divacancies are the only source of *random fields*, Figs. 1. All three curves in Figs. 1 exhibit changes in slope at about $T^{\bigstar} = T/T^0_{FE} \approx 0.22$, but these changes are smaller and less well defined than those in Figs. 2 and 3; suggesting that $T^{\bigstar}$ may mark either a continuous PNR⇌relaxor transition, or a crossover. Also, the erratic variations of order parameters, below $T^{\bigstar}$ that are evident in Figs. 2 and 3, are either undetectable within MD-precision, or absent in the NaCl-ordered system.

The rock-salt ordered relaxor has a very different microstructure Fig. 5 than the random- or nano-ordered cation configurations. In Fig. 5 Pb-displacement patterns and [Pb-O]-divacancy configurations are strongly correlated. Hence, even though the two panels represent a relaxor-, and a PNR-state that is close to T_B, their Pb-displacement patterns are strikingly similar; reflecting the pinning of Pb-displacement patterns to the [Pb-O]-divacancy configuration. Note that the polar microstructure of the rock-salt ordered system looks more like inter-penetrating, and percolating, +z and -z domains (out- and into the plane of the figure, respectively), than like ordered domains in a disordered matrix.

Random Chemical Disorder and the Nano-Ordered Configuration

Results for the random- and nano-ordered configurations exhibit very similar systematics for the $q_{\xi\xi}(T)$- and $q_{\Delta t}(T)$-curves with decreasing temperature: near T_B, there is a typically a broad minimum; between T_B and $T^{\bigstar}$, they increase smoothly and monotonically; at $T^{\bigstar}$, there appears to be a (weakly) first-order transition, Figs. 2 and 3; and below $T^{\bigstar}$, they vary erratically, and $q_{\Delta t}(T)$ evolves through local minima, Fig. 3b, before apparently converging. Also, there are strong correlations between chemical- and polar-order, Fig. 6 as reported in Burton *et al.* [18].

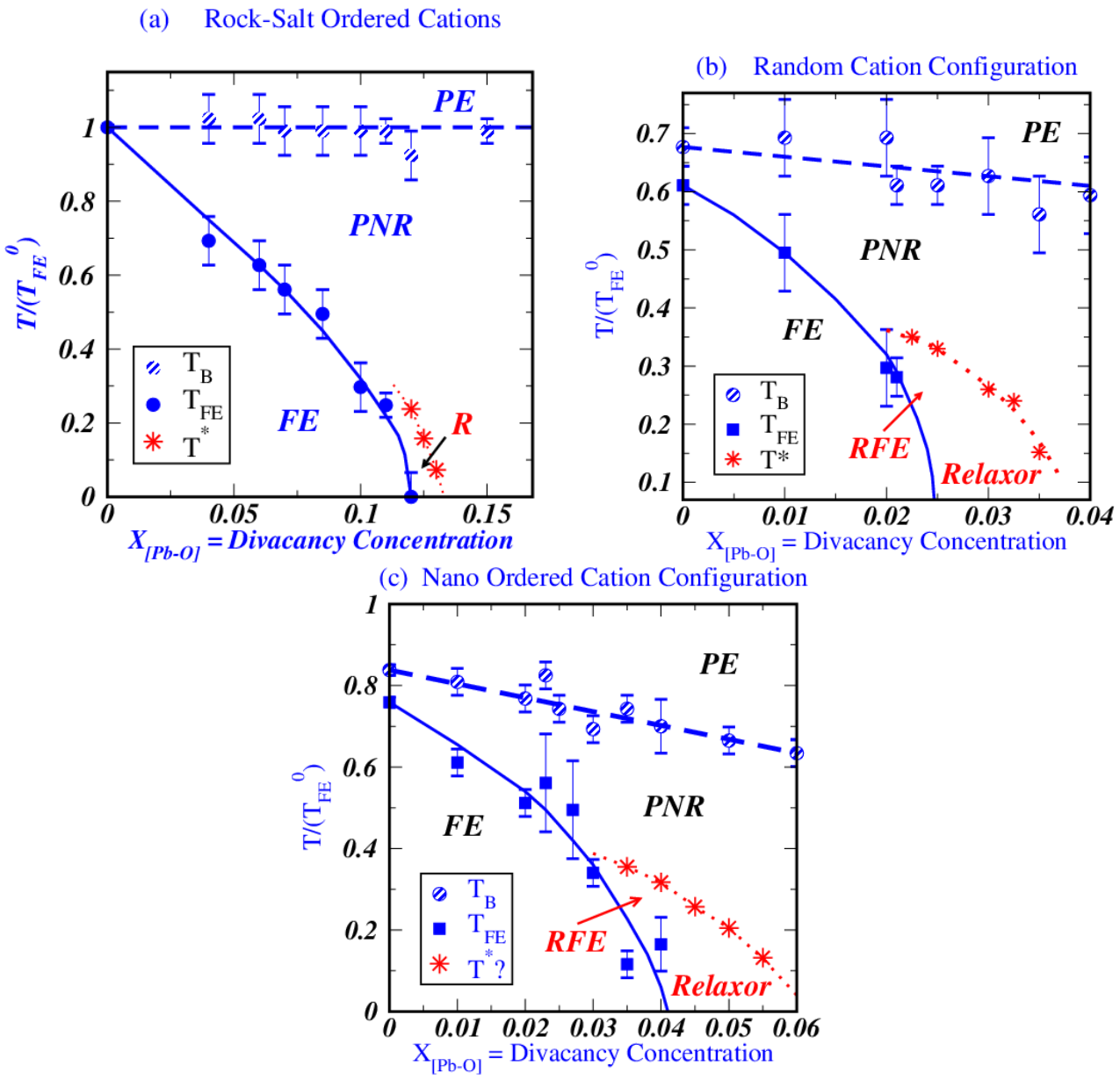

FIG. 4: Calculated $X_{[\mathrm{Pb-O}]}$ *vs.* T phase diagrams for the system $Pb_{1-X}(Sc_{1/2}Nb_{1/2})O_{3-X}$, with: a) ideal rock-salt type Sc:Nb-chemical order; b) a random Sc:Nb-cation configuration; c) a nano-ordered Sc:Nb-cation configuration, with ordered regions in a random matrix (25% ordered regions that are ≈2 nm in diameter). Labels: PE indicates a normal paraelectric; PNR indicates a system in which chemically ordered regions, with few $\vec{h_i}$, have higher polarization than the random matrix; FE indicates a ferroelectric ground-state; RFE indicates a relaxor-region above the FE-ground-state. Dashed lines (blue online) indicate Burns temperatures (T_B). Solid lines (blue online) indicate FE⇌PNR, or FE⇌RFE transitions. Dotted lines with large asterisk-symbols (red online) indicate RFE⇌PNR or relaxor⇌PNR transitions (crossovers).

DISCUSSION

Phase Diagram Topology

Notwithstanding the differences between $q_{\xi\xi}(T)$ and $q_{\Delta t}(T)$-curves for the NaCl-ordered configuration vs. those for the random- and NO-ordered configurations, all three phase diagrams exhibit the same topology, Figs. 4. Given that $X_{[\mathrm{Pb-O}]}$ and $\langle\vec{h_i}\rangle$ are interchangeable variables, the phase diagram topology exhibited in Figs. 4 can be taken

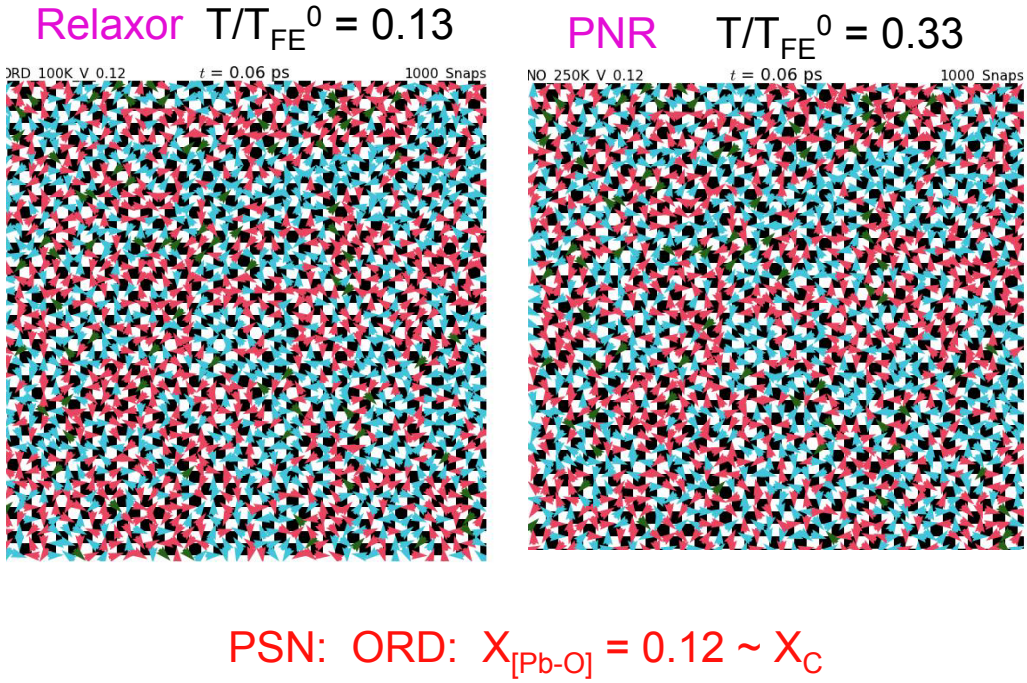

FIG. 5: MD-snapshots of the rock-salt ordered cation configuration black and white squares in the background indicate Sc- and Nb-ions, respectively. Pb-displacements in the relaxor- (left-panel) and PNR-regions (right panel) are plotted as fixed-length arrows: darker arrows (red online) indicate +z Pb-displacements (out of figure-plane); lighter arrows (blue online) indicate -z Pb-displacements (into figure-plane); large $<110>$-arrows (dark green online) indicate nn-$[Pb-O]$-divacancies. Both panels represent Pb-displacements after 1000 MD snapshots. Note how similar the +z/-z-configurations are in the two panels. This reflects the strong correlation between the [Pb-O]-divacancy configuration and the polar-microstructure over a wide T-range.

as a prototype for $Pb(B,B')O_3$ relaxor systems; as depicted in Fig.7. In Figs. 4, the RFE/relaxor field only occupies a narrow $X_{[\mathrm{Pb-O}]}$-range from about $X_C - 0.015$ to about $X_C + 0.025$; *i.e.* a limited range of average $\langle\vec{h_i}\rangle$-strength.

Comparison With Experiment

Given the approximations in this model, we do not expect *quantitative* accuracy in the calculated phase diagrams, but our results for a random cation configuration (Fig. 4b) agree reasonably well with experimental data of Chu et al. [3]. Their dielectric constant measurements of $\epsilon'(T)$ and $\epsilon''(T)$ for almost stoichiometric PSN $[Pb_{0.998}(Sc_{1/2}Nb_{1/2})O_{2.998}]$, and for PSN with $X_{[Pb-O]} = 0.017 \pm 0.003$ $[Pb_{0.983}(Sc_{1/2}Nb_{1/2})O_{2.983}]$, respectively, indicate that the former exhibits a first order $PNR \rightleftharpoons FE$ phase transition, while the latter, $Pb_{0.983}(Sc_{1/2}Nb_{1/2})O_{2.983}$, appears to exhibit fully relaxor behavior without an FE ground state. From Fig. 4b one correctly predicts the $PNR \rightleftharpoons FE$ phase transition in the $Pb_{0.998}(Sc_{1/2}Nb_{1/2})O_{2.998}$-sample, but one would expect the $Pb_{0.983}(Sc_{1/2}Nb_{1/2})O_{2.983}$-sample to also have a FE-ground-state, with an intermediate RFE-phase. In Fig. 4b, the calculated critical composition, beyond which there is no FE-ground state, is $X_C \approx 0.024$. This is at least half a percent larger than $Pb_{0.983}(Sc_{1/2}Nb_{1/2})O_{2.983}$ (the apparent *maximum* experimental value), which suggests that our model systematically underestimates the strength of random fields from charge disorder, vacancies, or both.

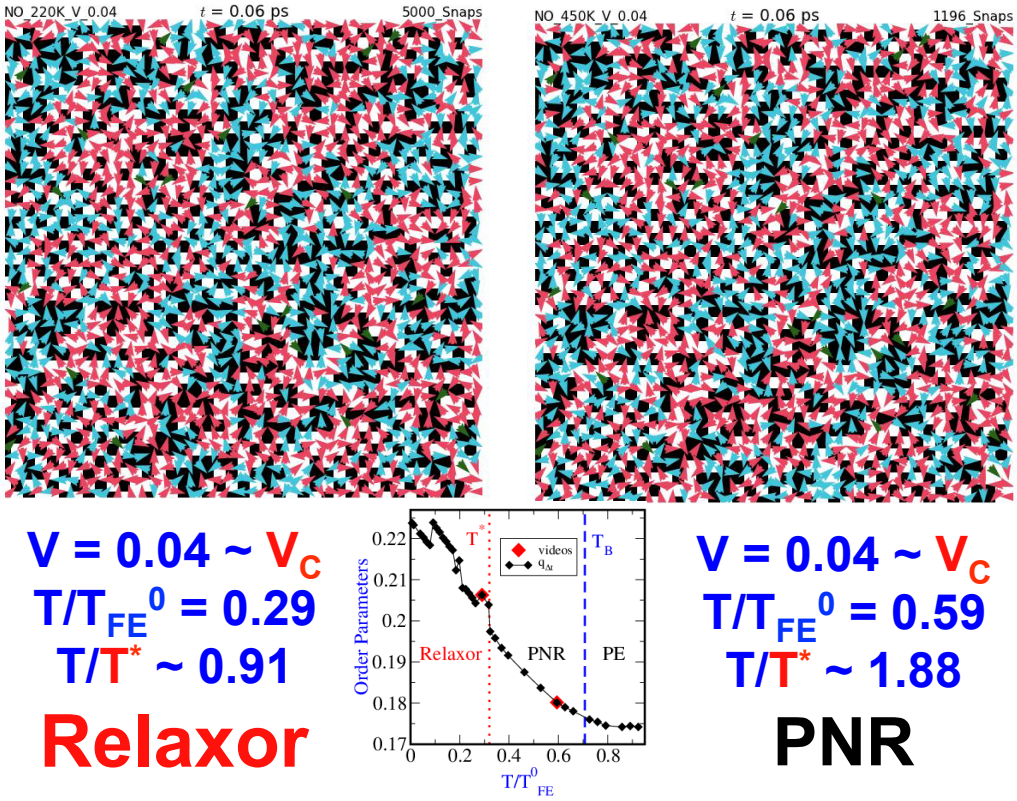

FIG. 6: MD-snapshots of the nano-ordered cation configuration after 5000 MD-snapshots, 50,000 MD time-steps: relaxor state is the left-panel, and PNR-state near-T_B is the right panel. Squares and arrows that describe the Sc:Nb-cation configuration and the Pb-displacements, respectively, are as in Fig. 5. Here chemically ordered- and disordered regions are evident, and there is a clear positive correlation between chemical- and polar-order. Also, as in the rock-salt ordered configuration, the +z/-z-configurations are strikingly similar, even though the relaxor- and PNR- snapshots are from very different temperatures (large diamonds in central panel, red online).

The PNR⇌relaxor transition and criticality

The apparent predictions of weakly first-order PNR⇌relaxor transitions in the random- and nano-ordered cation configurations has an important implication for relaxors. Specifically, a weakly first-order transition implies proximity to a critical point, and this suggests a simple explanation for the extraordinary electro-mechanical properties that are observed in relaxors; *i.e.* these properties diverge at a critical point, and are significantly enhanced close to a critical point. Indeed, Kutnjak *et al.*, attributed the giant electromechanical response in PMN-PT to a liquid-vapor like critical point. [28] The results reported here suggest that the PNR⇌relaxor transition is *typically* close to a critical point; e.g. *close*, in the sense that the application of a modest electrical field can drive the system from weakly first-order to critical.

Additional Phase Transitions?

The experimental phase diagram for the $Eu_XSr_{1-X}S$ exhibits a ferromagnetic⇌SG transition,[29] and in $Fe_{1-X}Au_X$ there are ferromagnetic⇌Mixed-phase- and SG⇌Mixed-phase-transitions [30]; in which, the Mixed-phase is ferromagnetic but replica-symmetry breaking (RSB) [26]. Compelling evidence of analogous transitions was not detected in this work [31], but such transitions are not ruled out, and there is clear similarity between relaxor- and magnetic spin-glass phase diagrams: Fig. 7 and Table I.

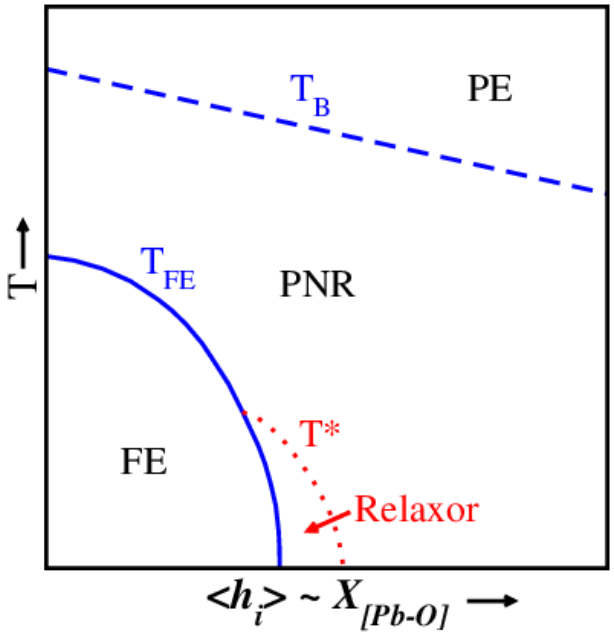

FIG. 7: Schematic prototype $\langle\vec{h_i}\rangle$ vs. T phase diagram for $Pb_{1-X}(B,B')O_{3-X}$ relaxor systems.

TABLE I: Relaxor vs. Magnetic Spin-Glass Analogy.

Relaxor	*Magnetic Spin − Glass*
$PE = paraelectric$	$PM = paramagnetic$
$PNR = Polar\ Nano\ Regions$	$SPM = superparamagnetic$
$FE = Ferroelectric$	$FM = Ferromagnetic$
$RSB = Replica - Symmetry - Breaking$	RSB
$RFE/relaxor$	$SG = SpinGlass$

CONCLUSIONS

The phase diagrams presented in Burton *et al.* [18] were incomplete because they omitted $T^{\bigstar}(X_{[\mathrm{Pb-O}]})$-curves; *i.e.* delineation of the RFE/relaxor-phase field. Results presented here include: calculations of $T^{\bigstar}(X_{[\mathrm{Pb-O}]})$-curves; suggest a prototype relaxor phase diagram topology; and strongly support the analogy between relaxors and magnetic spin-glasses, with respect to phase diagram topology, Table I.

The combination of soft-spins with explicit 1'st-3'rd nn-pairwise pseudospin-pseudospin interactions, 4'th-39'th nn dipole-dipole interactions, and random fields, is evidently sufficient to model heterovalent $Pb(B,B')O_3$ relaxor systems. Both the self-orvelap order parameter and the autocorrelation function appear to be good order parameters for locating $T^{\bigstar}(X_{[\mathrm{Pb-O}]})$-curves, and for demonstrating the glassy character of the relaxor-phase, which only occupies a narrow range in $X_{[\mathrm{Pb-O}]}$, or equivalently in $\langle\vec{h_i}\rangle$.

Previous conclusions [18, 19] about the strong correlation between chemically ordered regions and PNR are reinforced, with the addition that the orientations of PNRs become more static in the relaxor region, below the PNR⇌relaxor transition. In the random- and nano-ordered cation configurations $T^{\bigstar}$ appears to be a weakly first-

order transition, but results for the rock-salt ordered configuration are suggestive of a continuous transition or a crossover. Hence, chemical inhomogeneities such as chemical short-range order apparently amplify relaxor character.

ACKNOWLEDGEMENTS

B.P. Burton thanks D. Sherrington for inspiring this work and for helpful discussions.

[1] G. A. Smolensky and A. I. Agranovskaya, Sov. Phys. Sol. State **1**, 1429 (1959).
[2] L. E. Cross, Ferroelectrics **76**, 241 (1987).
[3] F. Chu, I.M. Reaney and N. Setter, J. Appl. Phys. **77**[4], 1671 (1995).
[4] F. Chu, N. Setter and A. K. Tagantsev, J. Appl. Phys. **74**[8], 5129 (1993).
[5] F. Chu, I.M. Reaney and N. Setter, J. Amer. Ceram. Soc. **78**[7], 1947 (1995)
[6] F. Chu, G. Fox and N. Setter, J. Amer. Ceram. Soc. **81**, (6) 1577 (1998)
[7] L. Bellaiche, J. Ìñiguez, E. Cockayne, and B. P. Burton Phys. Rev. B **75**, 014111 (2007).
[8] E. Cockayne and B. P. Burton, Phys. Rev. B **69**, 144116 (2004).
[9] W. Kleemann, J. Dec, V. V. Shvartsman, Z. Kutnjak and T. Braun, Phys. Rev. Lett. **97** 065702 (2006).
[10] J. Adv. Dielectrics **V2**, No. 2 1241001 (2012).
[11] B. P. Burton, E. Cockayne, S. Tinte and U. V. Waghmare, Phase Trans. **79**, 91 (2006).
[12] D. Sherrington Phys. Rev. Lett. **111**, 227601 (2013).
[13] D. Sherrington Phys. Rev. B **89**, 064105 (2014).
[14] D. Sherrington Physica Status Solidi b **251**, 1967 (2014).
[15] D. Sherrington Phase Transitions **88**, 202 (2015).
[16] S.F. Edwards, P.W. Anderson, J. Phys. F **5** 965 (1975).
[17] The phrase "quenched chemical disorder" implies that the chemical configuration is fixed within the temperature range that polar order-disorder is analyzed.
[18] B. P. Burton, E. Cockayne, S. Tinte and U. V. Waghmare, Phys. Rev. B **77**, 144114 (2008).
[19] B.P. Burton, E. Cockayne, S. Tinte, and U.V. Waghmare, Phys. Rev. B **72**, 064113 (2005).
[20] B. Dkhil, P. Femeiner, A. Al-Barakaty, L. Bellaiche, E. Dul'kin, E. Mojaev, and M. Roth, Phys. Rev. B **80** 064103 (2009).
[21] S. Tinte, B. P. Burton, E. Cockayne and U. V. Waghmare, Phys. Rev. Lett. **97**, 137601 (2006).
[22] W. Zhong, D. Vanderbilt and K. M. Rabe, Phys. Rev. Lett. **73**, 1861 (1994); K. M. Rabe and U. V. Waghmare, Phys. Rev. B **52**, 13236 (1995); U. V. Waghmare and K. M. Rabe, Phys. Rev. B **55**, 6161 (1997).
[23] U. V. Waghmare, E. Cockayne, and B. P. Burton, Ferroelectrics **291**, 187 (2003).
[24] B. P. Burton, U. V. Waghmare and E. Cockayne, TMS Letters, **1**, 29 (2004).
[25] G. Burns and F. H. Dacol, Solid State Commun. **48**, 853 (1983).
[26] T. Castellani and A. Cavagna J. Stat. Mecha. P05012 (2005) PII: S1742-5468(05)99356-4
[27] Fisher, M E (1998) Renormalization group theory: its basis and formulation in statistical physics, Reviews in Modern Physics **70**(2) 653-681.
[28] Z. Kutnjak, J. Petzelt and R. Blinc Nature **441** 956 (2006).
[29] H. Maletta and P. Convert, Phys. Rev. Lett. **42**, 108, (1979)
[30] R.B. Coles, B. Sarkissian, and R.H. Taylor, Phil. Mag. **B37**, 489 (1978)
[31] The strongest suggestion of such a transition is in the NO configuration where $q_{\Delta t}(t)$ exhibits a low-T reduction to a plateau, which does not seem to define a consistent phase-boundary or crossover (e.g. Fig. supplimentary material).